Ziploc-ing the structure 2.0: Endoplasmic reticulum-resident peptidyl prolyl isomerases show different activities toward hydroxyproline

Yoshihiro Ishikawa[‡§], **Kazunori Mizuno**[§1], and **Hans Peter Bächinger**[‡§2]

From the ‡*Department of Biochemistry and Molecular Biology, Oregon Health & Science University and* §*Research Department, Shriners Hospital for Children, Portland, Oregon 97239*

Edited by Amanda J. Fosang

Extracellular matrix proteins are biosynthesized in the rough endoplasmic reticulum (rER), and the triple-helical protein collagen is the most abundant extracellular matrix component in the human body. Many enzymes, molecular chaperones, and post-translational modifiers facilitate collagen biosynthesis. Collagen contains a large number of proline residues, so the *cis/trans* isomerization of proline peptide bonds is the rate-limiting step during triple-helix formation. Accordingly, the rER-resident peptidyl prolyl *cis/trans* isomerases (PPIases) play an important role in the zipper-like triple-helix formation in collagen. We previously described this process as "Ziploc-ing the structure" and now provide additional information on the activity of individual rER PPIases. We investigated the substrate preferences of these PPIases *in vitro* using type III collagen, the unhydroxylated quarter fragment of type III collagen, and synthetic peptides as substrates. We observed changes in activity of six rER-resident PPIases, cyclophilin B (encoded by the *PPIB* gene), FKBP13 (*FKBP2*), FKBP19 (*FKBP11*), FKBP22 (*FKBP14*), FKBP23 (*FKBP7*), and FKBP65 (*FKBP10*), due to posttranslational modifications of proline residues in the substrate. Cyclophilin B and FKBP13 exhibited much lower activity toward post-translationally modified substrates. In contrast, FKBP19, FKBP22, and FKBP65 showed increased activity toward hydroxyproline-containing peptide substrates. Moreover, FKBP22 showed a hydroxyproline-dependent effect by increasing the amount of refolded type III collagen *in vitro* and FKBP19 seems to interact with triple helical type I collagen. Therefore, we propose that hydroxyproline modulates the rate of Ziploc-ing of the triple helix of collagen in the rER.

Protein folding is a fundamental process in the cells, and a precisely folded protein is required to maintain homeostasis and physiological function in organisms. A large number of various types of molecular chaperones and enzymes exist to actively facilitate folding inside the cell (1, 2). Molecular chaperones provide substrates with a proper environment for folding intermediates containing hydrophobic surfaces that would otherwise aggregate (3). Enzymes recognize a certain amino acid or sequence to transform and bind to folding intermediates, which are termed isomerases and post-translational modifiers, respectively (4). They enhance the step-by-step folding to achieve a functional and mature protein. Collagen is the most abundant protein in human body, and its biosynthesis occurs in the rough endoplasmic reticulum (rER)[3] with >20 molecular chaperones and enzymes (5, 6). We named this network a "molecular ensemble," and it is an absolute requirement for the efficient folding and secretion of collagens (7). Collagen contains multiple G*XY* repeats, where *X* and *Y* are frequently occupied by proline and 4-hydroxyproline, respectively (8). Thus, collagen shows a unique amino acid composition with a large number of glycine and proline residues. In addition, some proline residues in *X* position are modified to 3-hydroxyproline (9). Three chains associate together to form an elongated helix with glycine residues in the inner core, called a triple helix. Formation of the triple helix is initiated at the carboxyl-terminal end in most types of collagen and proceeds toward the amino-terminal end in a zipper-like fashion wherein all proline peptide bonds have to turn into a *trans* state (10–12). The high proline content makes this isomerization of *cis* to *trans* the rate-limiting step for collagen folding; therefore, rER-resident peptidyl propyl *cis/trans* isomerases (PPIases) are involved in this step (13–16). In 2015, we reviewed the relationship of the rER-resident PPIases with collagen triple-helix formation and considered their roles during collagen folding (17). We termed this process "Ziploc-ing the structure" because the rER-resident PPIases coordinate the zipper-like fashion of collagen triple helix formation (17).

However, there are no data available to quantitatively compare the levels of enzymatic activities for individual rER-resident PPIases with a particular substrate. Especially, no reports exist on how PPIases behave when the proline-containing peptide substrates are hydroxylated. The FK506-binding protein (FKBP) family proteins contain at least one FKBP domain and

[3] The abbreviations used are: rER, rough endoplasmic reticulum; PPIase, peptidyl-prolyl *cis/trans* isomerase; CypB, cyclophilin B; FKBP, FK506-binding protein; Suc, succinyl; AMC, 7-amino-4-methylcoumarin; pNa, *p*-nitroanilide; IPTG, isopropyl 1-thio-*β*-D-galactopyranoside; DFP, diisopropyl fluorophosphate; *Z*, 3-hydroxyproline; BisTris, 2-[bis(2-hydroxyethyl)amino]-2-(hydroxymethyl)propane-1,3-diol.
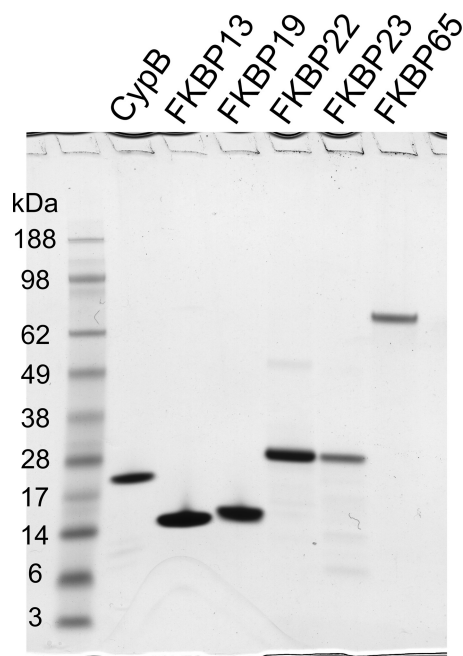
Figure 1. SDS-PAGE gel of purified rER-resident PPIases. The purified rER-resident PPIases were run on NuPAGE Novex BisTris 4–12% gel (Thermo Fisher Scientific) and stained with GelCode Blue Stain Reagent. Enzyme names shown are: CypB, recombinant chicken CypB; FKBP13, recombinant human FKBP13; FKBP19, the FKBP domain of recombinant human FKBP19; FKBP22, recombinant human FKBP22; FKBP23, recombinant human FKBP23; FKBP65, endogenous chicken FKBP65.

Table 1

The sequence comparison between FKBPs consisting of similar structural composition

The blue rectangles and orange ovals indicate the FKBP domain and EF-hand motif, respectively. Details are described under Experimental Procedures. FKBP19 is the FKBP domain of FKBP19 in this table.

	human		mouse	
	Consensus positions (%)	Identical positions (%)	Consensus positions (%)	Identical positions (%)
FKBP13 – FKBP19	54.5	41.5	54.5	43.1
FKBP22 – FKBP23	63.8	48.7	63.8	46.7

FKBP19 and FKBP22 and FKBP23 are shown in Table 1 and supplemental Fig. S1. Fig. 2 shows the CD spectra, and Table 2 describes the predicted secondary structure contents calculated from the CD spectra. To ensure whether the purified proteins folded properly, thermal transition curves were monitored by CD as a function of temperature. The thermal transitions in Fig. 2D show very sharp transitions around 65 °C for FKBP13 and FKBP19, indicating highly cooperative unfolding of the single domain. The transition of FKBP23 shows a broader transition at 60 °C. This could be due to the presence of the EF-hands in addition to the FKBP domain, a lower enthalpy change or folding intermediates. The transition of FKBP22 is even broader, probably due to the same reasons. Fig. 2, *D* and *E*, show that these proteins fold into a stable structure around physiological temperatures and the temperatures used in these experiments.

Both FKBP13 and the FKBP domain of FKBP19 consist of a single FKBP domain. Clear differences were shown in both the CD spectra and the predicted secondary structure (Fig. 2A and Table 2). Although the content of α-helix is similar, the FKBP domain of FKBP19 has more β-sheets and turns than FKBP13 (Table 2). The secondary structure of the FKBP domain of FKBP19 is similar to that of FKBP65 (Table 2). This could be reflected in the similarity of the CD spectra of the FKBP domain of FKBP19 that of FKBP65 reported previously (18). Both FKBP22 and FKBP23 are composed of one FKBP domain and two EF-hand motifs that bind to a calcium ion. Despite this common structure, they showed slightly different secondary structure contents (Table 2) and CD spectra (Fig. 2B). Some of the EF-hand motifs require a calcium ion to maintain the α-helical structure (19). The structure of FKBP23 changes after removing calcium (Fig. 2C), as was shown for FKBP22 previously (20). This suggests that the EF-hand motifs of FKBP22 and FKBP23 are calcium-sensitive structures in the rER. These CD analyses indicate that the FKBP domains can have different structures, which could influence their catalytic activity and substrate specificity.

Classical molecular chaperone assay of FKBP13, the FKBP domain of FKBP19, and FKBP23 and their interaction with type I collagen

To assess the molecular chaperone activity of FKBP13, the FKBP domain of FKBP19, and FKBP23, we performed two biochemical assays *in vitro*. Because molecular chaperone activities have been already measured for CypB, FKBP65, and FKBP22 (18, 20, 21), we investigated the chaperone function of

have PPIase activity and/or chaperone activity (17). This domain is identified by a certain profile of amino acid sequences (prosite). However, the structure-function relationship of this domain is not well established. In this report we measured the circular dichroism (CD) spectra to investigate the structural comparison between FKBPs composed of similar domains and performed *in vitro* enzyme assays to evaluate the chaperone and isomerase activities of six rER-resident PPIases: cyclophilin B (CypB), FKBP13, FKBP19 (only the FKBP domain), FKBP22, FKBP23, and FKBP65. We also show the PPIase activities toward hydroxyproline-containing substrates and compare differences observed between proline- and hydroxyproline- containing substrates.
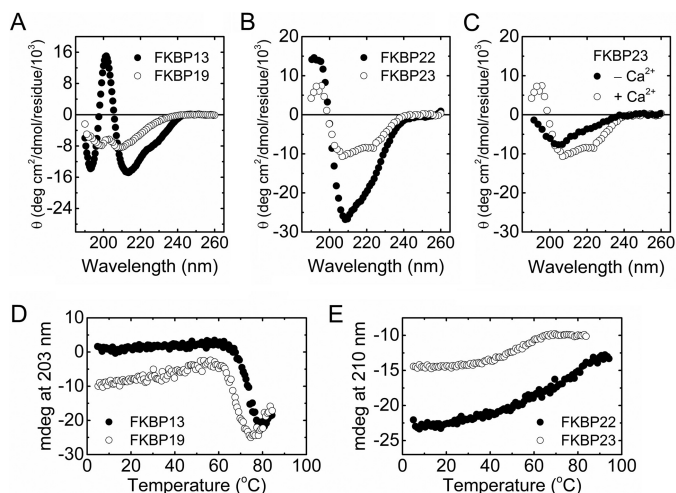
Results and discussion

Basic characterizations of purified rER-resident PPIases

Fig. 1 shows an SDS-polyacrylamide gel of purified rER-resident PPIases under reducing conditions. The purified FKBP13 (123 amino acids and 13444.5 Da) and FKBP domain of FKBP19 (121 amino acids and 13054.9 Da) are expected to have a similar migration on the SDS-polyacrylamide gel; however, FKBP13 (*second lane* in Fig. 1) migrates slightly faster than the FKBP domain of FKBP19 (*third lane* in Fig. 1). This might be caused by the difference in the theoretical pI between 8.93 for FKBP13 and 4.80 for the FKBP domain of FKBP19 (theoretical pIs were calculated using the ProtParam tool provided from ExPASy. In contrast, FKBP22 (200 amino acids, 22845.9 Da, pI 5.28) and FKBP23 (208 amino acids, 23820.7 Da and pI 5.27) migrate similarly (*fourth* and *fifth lanes* in Fig. 1). A sequence comparison and alignment between FKBP13 and the FKBP domain of

Figure 2. Circular dichroism measurements of FKBPs. The wavelength scan and thermal transition were measured using circular dichroism. *A*, the wavelength spectra of recombinant human FKBP13 (*filled circle*) and FKBP domain of recombinant human FKBP19 (*open circle*). *B*, the wavelength spectra of recombinant human FKBP22 (*filled circle*) and recombinant human FKBP23 (*open circle*). *C*, the wavelength spectra of recombinant human FKBP23 in presence (*filled circle*) or absence (*open circle*) of calcium. *D*, the thermal transition curves of recombinant human FKBP13 (*filled circle*) and FKBP domain of recombinant human FKBP19 (*open circle*). *E*, the wavelength spectra of recombinant human FKBP22 (*filled circle*) and recombinant human FKBP23 (*open circle*). The FKBP domain of FKBP19 is indicated as FKBP19 in the figures.

Table 2

**Comparison of the secondary structure content of the rER resident FKBPs**

FKBP	α-Helix	β-Sheets	Irregular	Reference
Human FKBP13[a]	0.00	0.43	0.57	
	0.06	0.4	0.53	PDB code 4NNR
Human FKBP19[b]	0.09	0.29	0.61	
Human FKBP22[a]	0.29	0.21	0.5	
	0.27	0.29	0.44	PDB code 4MSP[c]
Human FKBP23	0.15	0.23	0.61	
Chicken FKBP65	0.12	0.29	0.59	

[a] The numbers of in the lower row were calculated by Stride Services using the PDB file shown in reference.
[b] Human FKBP19 is the FKBP domain of FKBP19 in this table.
[c] From Ref. 55.

FKBP13, the FKBP domain of FKBP19, and FKBP23. First, we tested a classical molecular chaperone assay, the thermal aggregation of citrate synthase. Only the FKBP domain of FKBP19 prevented aggregation of citrate synthase (Fig. 3*A*) and showed concentration-dependent inhibition (Fig. 3*B*). However, this chaperone activity was smaller compared with the positive control PDI (Fig. 3, *A* and *B*). Next, to evaluate whether these three FKBPs are involved in collagen quality control, we measured the effect on collagen fibril formation. When collagens are folded into a triple helix in the rER the stability of this newly formed structure is stabilized by the chaperones Hsp47 and FKBP65. This interaction also helps to prevent premature aggregation of these molecules. FKBP13 and FKBP23 did not affect the fibril formation of type I collagen (Fig. 3*C*). In contrast, in the presence of the FKBP domain of FKBP19 fibril formation of type I collagen was delayed (Fig. 3*C*), and this delay became larger with increasing concentrations of the FKBP domain of FKBP19 (Fig. 3*D*). Likewise, the activity was not only much weaker than the positive control decorin (22), but also FKBP65, as previously reported (18). As we described above,
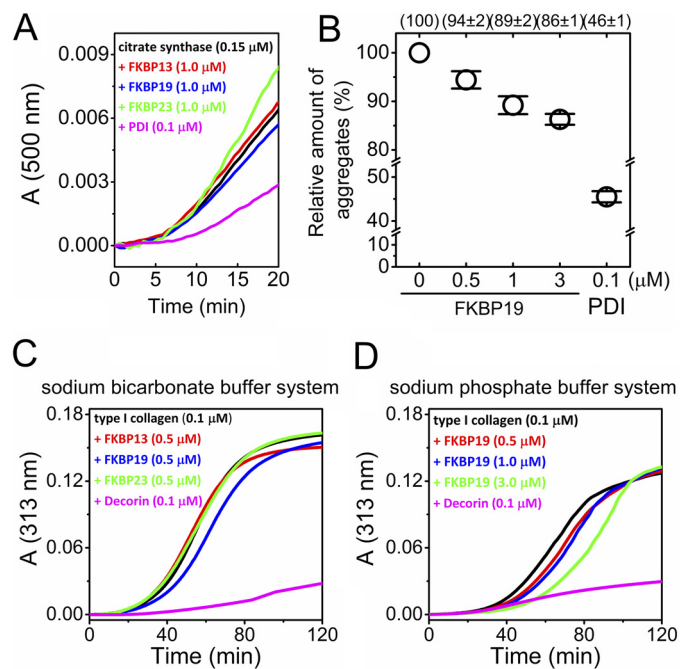
Figure 3. Molecular chaperone function of FKBPs. *A* and *B* show the classical chaperone activity assay using the thermal aggregation of citrate synthase. The assay was monitored at 500 nm, and 30 μM citrate synthase solution was diluted 200-fold into prewarmed 40 mM HEPES buffer, pH 7.4, containing 1 mM CaCl₂ at 43 °C. *A*, in the absence (*black*) and presence (*red*) of recombinant human FKBP13, recombinant human FKBP domain of FKBP19 (*blue*), and recombinant human FKBP23 (*green*). The protein concentration was 1.0 μM for these FKBPs. 0.1 μM PDI was used as a positive control (*magenta*). All curves are averaged by a minimum of three measurements. *B*, results are shown as the percentage of inhibitions of thermal aggregation of citrate synthase with 0.5, 1.0, and 3.0 μM concentrations of the FKBP domain of FKBP19. The amount of aggregates generated without the FKBP domain of FKBP19 was set as 100%, and 0.1 μM PDI is shown as a comparison. Each data point was calculated by a minimum of three measurements using three independent experiments. *C* and *D* show the fibril formation of type I collagen. A stock solution of type I collagen in 50 mM acetic acid was diluted to a final concentration of 0.1 μM. *C*, the measurements were performed in 0.1 M sodium bicarbonate buffer, pH 7.8, containing 0.15 M NaCl and 1 mM CaCl₂ at 34 °C. Shown in the absence (*black*) and presence (*red*) of recombinant human FKBP13, recombinant human FKBP domain of FKBP19 (*blue*), and recombinant human FKBP23 (*green*). The protein concentration was 0.5 μM for these FKBPs. 0.1 μM decorin was used as a positive control (*magenta*). All curves are averaged by a minimum of three measurements. *D*, the measurements were performed in 0.15 M sodium phosphate buffer, pH 7.8, containing 0.15 M NaCl at 34 °C. Shown is the absence (*black*) and presence (*red*) of 0.5 μM, 1.0 μM (*blue*), and 3.0 μM (*green*) recombinant human FKBP domain of FKBP19. 0.1 μM decorin was used as a positive control (*magenta*). All curves are averaged by a minimum of three measurements. The FKBP domain of FKBP19 is indicated as FKBP19 in the figures.

FKBP65 and FKBP19 showed similar CD spectra (Fig. 2*A*, Table 2, and Ref. 18) and marginally acted as a molecular chaperone (Fig. 3 and Ref. 18). This suggests that the FKBP domains of FKBP19 and FKBP65 may have similar structural features.

Determination of the isomerase activity of the γ PPIases using type III collagen and peptide substrates

The collagen triple helix is formed in a zipper-like fashion, and this folding is accelerated by PPIases. Three rER-resident PPIases, CypB, FKBP65, and FKBP22, were shown to influence the rate of type III collagen refolding *in vitro* (18, 20, 21, 23). However, it is difficult to compare the level of their activities directly because different experimental conditions were used. Other rER-resident PPIases like FKBP13, FKBP19, and FKBP23

Non-hydroxylated type III collagen quarter fragment (2.0 μM)

Full length native type III collagen (0.2 μM)
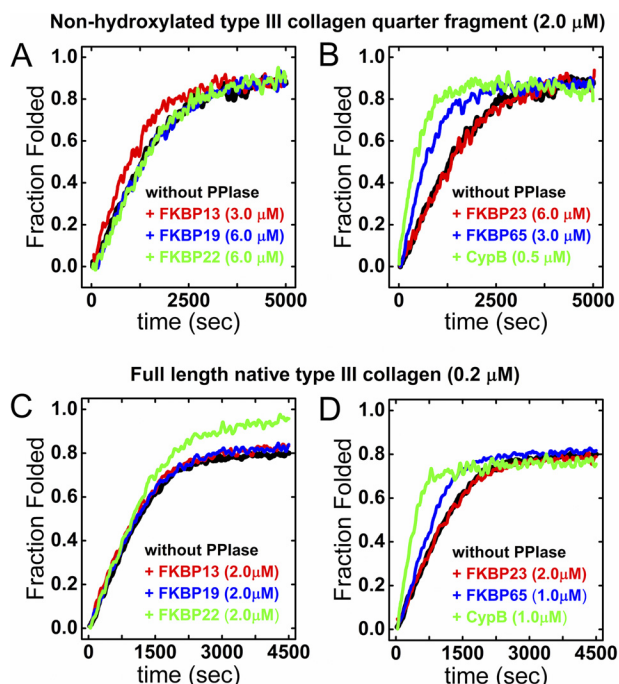
Figure 4. Refolding of the carboxyl-terminal quarter fragments of type III collagen without prolyl 4-hydroxylation and full-length type III collagen. Kinetics of the refolding of the carboxyl-terminal quarter fragment of type III collagen without prolyl 4-hydroxylation (final concentration 2.0 μM) and full-length type III collagen (final concentration 0.2 μM) in the presence of the rER-resident PPIases monitored by CD at 220 nm is shown. The protein concentrations used were 3.0 μM and 2.0 μM for FKBP13, 6.0 μM and 2.0 μM for the FKBP domain of FKBP19, FKBP22, and FKBP23, 3.0 μM and 1.0 μM for FKBP65, and 0.5 μM and 1.0 μM for CypB for the carboxyl-terminal quarter fragment of type III collagen without prolyl 4-hydroxylation and full-length type III collagen, respectively. All curves are averaged by a minimum of three measurements. *A–B* and *C–D* indicate the refolding of the carboxyl-terminal quarter fragments of type III collagen without prolyl 4-hydroxylation and the refolding of full-length type III collagen, respectively. The absence of PPIases is shown as *black* in *A–D*. The presence of PPIases is annotated in individual figures using *red*, *blue*, and *green*. The FKBP domain of FKBP19 is indicated as FKBP19 in the figures.

could possibly be involved in collagen folding. Therefore, we tested two enzyme assays using type III collagen and short peptides as substrates to address the effect on collagen folding and the individual level of PPIase activity among six rER-resident PPIases.

We prepared two different collagen substrates with and without prolyl 4-hydroxylation and measured type III collagen refolding using CD. The CD signal reflects the rate of collagen refolding from a denatured state because PPIases are stable around physiological temperatures (Fig. 2, *D* and *E*), and the CD signals of the PPIases are not changed during the measurements. Two PPIases, the FKBP domains of FKBP19 and FKBP23, did not affect the rate of refolding for either substrate, whereas the other two PPIases, CypB and FKBP65, increased the rate of folding for both (Fig. 4, *B* and *D*). CypB had the highest activity for both substrates but did not enhance the amounts of refolded type III collagen (Fig. 4, *B* and *D*). On the other hand, FKBP22 clearly improved formation of folded molecules (Fig. 4*C*), and this observation was reported before (20). The reason for this increase is not currently understood but could be due to specific sequences in type III collagen, and we will investigate this further in the near future. Higher con-

centrations of FKBP65 were required to detect activity (Fig. 4*B*), which corresponds to the marginal effect on type III collagen refolding shown previously (24). One interesting observation is the prolyl 4-hydroxylation-dependent difference in substrate recognition between FKBP13 and FKBP22 (Fig. 4). FKBP13 recognizes the unhydroxylated type III collagen but not the hydroxylated collagen, whereas the opposite is true for FKBP22. The increase in the rate of folding of unhydroxylated type III collagen in Fig. 4*B* is with a lower concentration of CypB (0.5 μM) compared with the concentration of other PPIases (3–6 μM). The concentration of CypB in Fig. 4*D* is 1.0 μM compared with 1–2 μM for the other PPIases. This shows that CypB prefers unhydroxylated type III collagen as a substrate.

Next, we quantitated the level of activity using peptide substrates in a stopped-flow system with an established procedure (25–27). We prepared not only short peptides containing proline residues but also peptides containing prolyl 3- and 4-hydroxylation. The general trends in this assay corresponded to the result of type III collagen refolding, and the calculated k_{cat}/K_m values are shown in Table 3 and Fig. 5. CypB has the highest catalytic activity, and FKBP65 shows decent activities among the six PPIases toward all seven peptide substrates. CypB shows a decreased activity for hydroxyproline-containing peptides; however, CypB still has the highest activity among the six PPIases (see Table 3). The substrate recognition of FKBP13 and FKBP22 depends on the prolyl 4-hydroxylation as found in the type III collagen refolding assay. It is interesting to note that AMC peptides showed larger k_{cat}/K_m values than *p*-nitroanilide (pNa) peptides despite that the concentration of pNa peptides were higher than that of AMC. Additionally, the order of level of activity was slightly altered between AMC and pNa. These compounds may affect the efficiency of the association and the dissociation with the substrate and also of the chymotrypsin activity. However, overall trends of level of PPIase activities are comparable.

The catalytic activities of PPIases are influenced by posttranslational modifications

Two novel observations are found in studies using peptide substrates with and without hydroxyproline. First, FKBP13 and CypB showed a much lower activity toward hydroxylated substrates. Second, the FKBP domain of FKBP19, FKBP22, and FKBP65 overall preferred hydroxylated substrates (Table 3 and Fig. 5). Although CypB still showed high level of activities for both hydroxylated type III collagen and peptide substrates, prolyl hydroxylation reduced the activity of CypB. FKBP13 also preferred the unhydroxylated peptides as substrates (Fig. 4, Fig. 5, and Table 3). Prolyl 4-hydroxylation is required to provide thermal stability to the collagen triple helix (28–30); therefore, "Ziploc-ing" will not proceed unless prolyl 4-hydroxylations are completed. Indeed, collagen prolyl 4-hydroxylase I, coded in *P4HA1* gene, null mice are embryonic lethal (31). Here, we propose that prolyl 4-hydroxylation also provides selective substrates for the rER-resident PPIases during collagen triple helix formation. As a consequence, whereas Gidalevitz *et al.* (2) briefly mentioned that FKBP13 knock-out mice did not have an obvious phenotype, human mutations in the *PPIB* and *FKBP14* gene, encoding CypB and FKBP22, and the absence of these

Table 3

The PPIase activities of rER resident PPIases with Suc-A*XY*F-pNa /AMC peptides as substrates

O and *Z* indicate 4-hydroxyproline and 3-hydroxyproline, respectively. The results are shown as a mean ± S.D.

| | k_{cat/K_m} | | | | | | | | |
| | Suc-A*XY*F-pNa | | | | | | | Suc-A*X*PF-AMC | |
PPIease	-*AP*-	-*AO*-	-*LP*-	-*LO*-	-*GP*-	-*GO*-	-*GZ*-	-*AP*-	-*LP*-
	$(mM^{-1} \cdot s^{-1})$							$(mM^{-1} \cdot s^{-1})$	
Human FKBP13	41.0 ± 3.7	1.47 ± 0.85	620 ± 46	77.6 ± 23.1	2.7 ± 1.6	9.68 ± 4.41	3.68 ± 2.88	383.5 ± 78.4	1711 ± 340
Human FKBP19[a]	0.23 ± 0.18	8.41 ± 2.79	0.59 ± 0.12	64.5 ± 36.1	0.36 ± 0.17	9.48 ± 4.41	9.66 ± 2.62	1.35 ± 0.62	35.9 ± 19.1
Human FKBP22	1.13 ± 0.75	14.7 ± 3.2	0.45 ± 0.09	17.6 ± 7.3	0.23 ± 0.14	21.8 ± 13.4	81.1 ± 31.5	1.3 ± 0.8[b]	30.7 ± 12.5[b]
Human FKBP23	1.36 ± 0.91	2.31 ± 1.2	0.87 ± 0.41	9.75 ± 4.8	1.44 ± 0.12	0.87 ± 0.4	18.3 ± 4.4	14.5 ± 6.0	63.0 ± 14.8
Chicken FKBP65	15.6 ± 1.6	38.1 ± 5.5	8.17 ± 2.59	30.7 ± 8.6	7.24 ± 4.6	24.4 ± 9.6	20.4 ± 12.3	232[c]	370 ± 66
Chicken CypB	10839 ± 699	217 ± 24	2516 ± 74	117 ± 60	3178 ± 393	49.6 ± 36	111 ± 36	23,270 ± 5000[b]	7900 ± 400[b]

[a] Human FKBP19 is the FKBP domain of FKBP19 in this table.

[b] From Ref. 20.

[c] From Ref. 24.
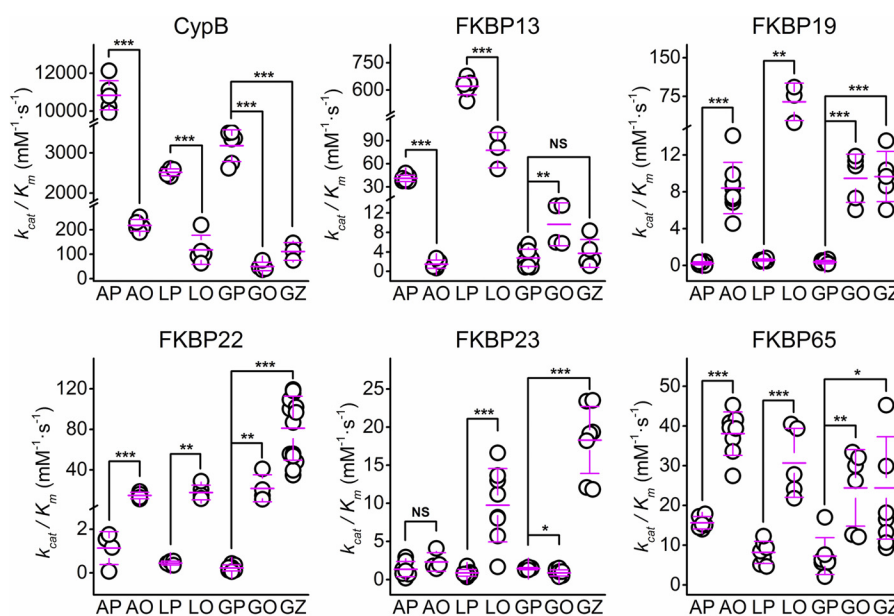
Figure 5. Catalytic efficiency for the prolyl isomerization using pNa peptide substrates. The catalytic efficiency (k_{cat}/K_m) for the isomerization reaction was determined by kinetic measurements using the Suc-Ala-*XY*-Phe-pNa peptide substrates, where *XY* indicates the combination of two amino acids labeled in graphs. The enzymatic activity of prolyl isomerization of seven peptide substrates for six PPIases, including the mean ± S.D. as a *magenta line* derived from Table 3, is indicated. The *p* value is annotated as follows (*, $p < 0.05$; **, $p < 0.005$; ***, $p < 0.0005$. *NS*, not significant). The FKBP domain of FKBP19 is indicated as FKBP19.

proteins result in connective tissue disorders osteogenesis imperfecta and Ehlers-Danlos syndrome (32–35). In contrast to prolyl 4-hydroxlation, the function of prolyl 3-hydroxylation in collagens is not clearly understood. From studies of osteogenesis imperfecta, it is proposed that prolyl 3-hydroxylation is required for collagen-protein interactions and the cell-matrix signaling pathways. Reduced binding of collagen to small leucine-rich proteoglycans and increased transforming growth factor-β signaling was observed (36). Prolyl 3-hydroxylation seems to occur only in the *X* position proline in the *GXO* collagenous sequence, where "*O*" indicates 4-hydroxylproline, and the amount of prolyl 3-hydroxylation depends on the type of collagen (9, 37, 38). For example, type IV collagen contains the largest number of prolyl 3-hydroxylation (39–41), but there is no 3-hydroxyproline in type III collagen (9). Our peptide assays demonstrate that the *GZ* peptide, where "*Z*" indicates 3-hydroxyproline, is a better substrate than the GP peptide except for FKBP13 and CypB. CypB forms a tight complex with prolyl 3-hydroxylase 1 and cartilage-associated protein (CRTAP) (42).

This complex is responsible for the important 3-hydroxylation of α1-Pro986 in type I collagen. The absence or mutations in any individual member of this complex leads to osteogenesis imperfecta with an impaired folding of the type I collagen triple helix, even in presence of free active CypB in the rER (43–48). The prolyl 3-hydroxylase 1 (P3H1)-cartilage-associated protein (CRTAP)-CypB complex not only has prolyl 3-hydroxylase activity but also stabilizes the newly formed triple helix and likely helps localize CypB to its substrate. A large number of molecules interact with these rER-resident PPIases (see Table 1 in Ref. 17). These interactions expand the repertoire of functions of rER-resident PPIases.

Another observation is that there are sequence preferences in the molecular recognition of PPIases. The prolyl isomerase activity depends on the amino acid preceding proline (Fig. 5, Table 3, and Refs. 24 and 26). FKBP13 shows a significant reduction of its activity to GP-containing substrate compared with other amino acids (Fig. 5 and Table 3). Prolyl 3-hydroxylation did not change the activity of FKBP13, but a slight

increase in activity was observed with 4-hydroxyproline (Fig. 5 and Table 3). This result provides an explanation why FKBP13 is not involved in collagen folding because in collagens the *X* position in G*XY* sequence is frequently occupied by proline but not 4-hydroxyproline (8).

It was proposed that FKBP22 could recognize 4-hydroxyproline-containing substrates preferentially (20), however there was no direct evidence. Here, we tested the direct influence of prolyl 4-hydroxylation on the activity of FKBP22 using peptide substrates. FKBP22 does show increased activity for hydroxyproline peptides. Surprisingly, the FKBP domain of FKBP19 also shows increased levels of activity for hydroxyproline in the peptide assays (Fig. 5 and Table 3). But the FKBP domain of FKBP19 does not act as a catalyst in the native type III collagen refolding assay (Fig. 4*C*). The FKBP domain of FKBP19 showed little activity toward GP- and *X*P-containing substrates. The highest activity was observed for the LO peptide. Although GP sequences frequently appear in collagen (32.9%), LO sequences are rare (7.8%) (8). This is probably the reason why there was no effect in the presence of the FKBP domain of FKBP19 during full-length native type III collagen folding despite increased activity toward hydroxyproline peptides. In addition, FKBP22 was also the only enzyme that showed an increase in the amount of refolded type III collagen (Fig. 4*C*). This suggests that FKBP22 may have a unique capability of molecular and/or sequence recognition. This could explain as well that FKBP22 bound to type III, VI, and X collagen but not to types I, II, and V collagen (20). FKBP23 showed low but measurable activities toward peptide substrates (Fig. 5 and Table 3). FKBP23 itself was folded and stabled around physiological temperatures (Fig. 2*E*). We only tested three combinations of amino acids next to proline (Ala, Leu, and Gly), which appear with different frequencies in collagen sequences (8). It is possible that FKBP23 preferentially catalyzes other amino acids or complex formation is required with other molecular chaperones for optimal activity.

Elastin, which is also an extracellular matrix protein biosynthesized in the rER, was shown to have hydroxyproline (49). Isomerization of a conserved proline residue in the C_H1 domain of IgG molecules is essential for their folding, assembly, and secretion (50). Other proteins with proline-rich regions (51, 52) might require PPIases for correct folding. Therefore, PPIases play an important role not only for collagen but also non-collagenous molecules during their folding, and differences in PPIase activities may determine folding pathways of these molecules.

In summary, we show that some PPIases have preferences for post translationally modified proline residues as substrates and that prolyl 4-hydroxylations not only provide thermal stability to collagen triple helices but also modulate the rate of Ziplocing of the triple helix of collagen in the rER.

Experimental procedures

Cloning, expression, and purification of human recombinant FKBP13

FKBP2 encoding FKBP13 human cDNA Clone (catalogue #SC120228) was purchased from Origene Technologies. The FKBP13 protein coding sequence without the signal peptide

was isolated from the cDNA by PCR with primers containing a BamHI site at the 5′ end and a SalI site after the stop codon at the 3′ end. That DNA was inserted of a pET30a(+) expression vector (Thermo Fisher Scientific). The expression vectors were transformed into *Escherichia coli* BL21(DE3) and grown at 37 °C to an optical density of 0.6 at 600 nm with 2× TY medium (Sigma-Aldrich). Proteins were induced by 1 mM isopropyl 1-thio-β-D-galactopyranoside (IPTG) at 15 °C overnight. The cells were harvested by centrifugation and resuspended in B-PER (Thermo Fisher Scientific). 30% (w/v) of ammonium sulfate was added to the soluble fraction, and the supernatant after centrifugation was passed through a 0.22-μm filter and loaded onto Ni^{2+}-chelating column. After washing with 40 mM Tris/HCl buffer, pH 7.5, containing 0.5 M NaCl and 20 mM imidazole (minimum 5 column volume), FKBP13 was eluted with 40 mM Tris/HCl buffer, pH 7.5, containing 0.5 M NaCl and 500 mM imidazole. The fractions containing FKBP13 were dialyzed into 50 mM Tris/HCl, pH 8.0, containing 1 mM $CaCl_2$ and 0.05% Tween 20, and then enterokinase (0.5 units/ml reaction volume) (Life Technologies, Inc.) was used to cleave the His tag at 4 °C overnight. After dialysis into the same Tris/HCl buffer used for the chelating column before, the solution was applied onto a Ni^{2+}-chelating column to remove the His-tag fragment, and the flow-through fraction that includes FKBP13 was treated with 1 μl/ml diisopropyl fluorophosphates (DFP) to inactivate proteases derived from *E. coli* and gently stirred for 4 h on ice. After treatment, the protein solution was dialyzed against 20 mM HEPES, pH 7.4, and loaded onto a HiTrap SP FF column (GE Healthcare), and FKBP13 was eluted with 200 mM NaCl. The purified FKBP13 was dialyzed against different reaction buffers and used for further experiments.

Cloning, expression, and purification of FKBP domain of human recombinant FKBP19

FKBP11 encoding FKBP19 human cDNA (clone ID: HsCD00021579) was purchased from Harvard Medical School (PLASMID). The FKBP domain of FKBP19-coding sequence without the signal peptide (between Gly-28 and Ala-146) was isolated from the cDNA by PCR with primers containing a BamHI site at the 5′ end and a SalI site at the 3′ end. That DNA was inserted to a pET30a(+) expression vector. The expression vectors were transformed into *E. coli* BL21(DE3) and grown at 37 °C to an optical density of 0.6 at 600 nm with 2× TY medium. Proteins were induced by 1 mM IPTG at 15 °C overnight. The cells were harvested by centrifugation and resuspended in B-PER. The soluble fraction was passed through a 0.22-μm filter and loaded onto Ni^{2+}-chelating column. After the column was washed with 40 mM Tris/HCl buffer, pH 8.2, containing 0.5 M NaCl and 20 mM imidazole (minimum 5 column volumes), the FKBP domain of FKBP19 was eluted with 40 mM Tris/HCl buffer, pH 8.2, containing 0.5 M NaCl and 500 mM imidazole. The fractions containing the FKBP domain of FKBP19 were dialyzed into 50 mM Tris/HCl, pH 8.0, containing 1 mM $CaCl_2$ and 0.05% Tween 20. Enterokinase (0.5 units/ml reaction volume) was used to cleave the His tag at 4 °C overnight, and the sample was treated with 1 μl/ml DFP to inactivate proteases derived from *E. coli* and gently stirred for 4 h on ice. Buffer exchange and the removal of contaminating proteins

was done on a HiTrapQ XL column (GE Healthcare), and the FKBP domain of FKBP19 was eluted with 40 mM Tris/HCl buffer, pH 7.5, containing 0.5 M NaCl and 10 mM imidazole. This eluted fraction was directly applied onto a Co^{2+}-chelating column to remove the His-tag fragment. The flow-through fraction included the FKBP domain of FKBP19 and was dialyzed against 40 mM Tris/HCl buffer, pH 7.0, containing 1.0 M ammonium sulfate, loaded onto a HiTrap Phenyl HP column (GE Healthcare Life Sciences), and eluted with a liner gradient from 1.0 M to 0 M ammonium sulfate. Purified FKBP domain of FKBP19 was dialyzed against different reaction buffers to remove ammonium sulfate and used for further experiments.

Cloning, expression, and purification of human recombinant FKBP23

FKBP7 encoding FKBP23 human cDNA (human MGC verified full-length cDNA, clone ID: 3891173) was purchased from Thermo Fisher Scientific. The FKBP23 protein-coding sequence without the signal peptide was isolated from the cDNA by PCR with primers containing an EcoRI site at the 5′ end and a XhoI site after the stop codon at the 3′ end. That DNA was inserted to a pET30a(+) expression vector. The expression vectors were transformed into *E. coli* BL21(DE3) and grown at 37 °C to an optical density of 0.6 at 600 nm with LB medium. Proteins were induced by 1 mM IPTG at 20 °C overnight. The cells were harvested by centrifugation and resuspended in Tris-based B-PER containing 1 mM $CaCl_2$. 30% (w/v) of ammonium sulfate was added to the soluble fraction and incubated for 30 min for room temperature. The precipitated materials after centrifugation were dissolved into 20 mM HEPES buffer, pH 7.5, containing 1.0 M NaCl, 20 mM imidazole, 1 mM $CaCl_2$, and 1.0 M urea. After removing undissolved materials by centrifugation, the protein solution was passed through a 0.22-μm filter and loaded onto Co^{2+}-chelating column. After the column was washed with the same buffer used for resuspending of the pellets of the ammonium sulfate precipitation (minimum 5 column volume), FKBP23 was eluted with 20 mM HEPES buffer, pH 7.5, containing 1.0 M NaCl, 500 mM imidazole, 1 mM $CaCl_2$, and 1 M urea. The fractions containing FKBP23 were dialyzed into 50 mM Tris/HCl, pH 8.0, containing 1 mM $CaCl_2$ and 0.05% Tween 20, and then enterokinase (1.0 units/ml reaction volume) was used to cleave the His tag at 4 °C overnight. After dialyzing into the same HEPES buffer used for washing the chelating column, solution was treated with 1 μl/ml DFP to inactivate proteases derived from *E. coli* and gently stirred for 4 h on ice. The protein solution was applied onto a Co^{2+}-chelating column to remove the His-tag fragment. The flow-through fraction including FKBP23 was dialyzed against 20 mM triethanolamine/HCl buffer, pH 7.5, containing 20 mM NaCl, 1 mM $CaCl_2$, and 1.0 M urea and loaded onto a HiTrapQ XL column. Contaminants and clean FKBP23 were eluted with 20 and 30% of 20 mM triethanolamine/HCl buffer, pH 7.5, containing 500 mM NaCl, 1 mM $CaCl_2$, and 1.0 M urea, respectively. The purified FKBP23 was dialyzed against different reaction buffers to remove urea and used for further experiments.

Purification of human FKBP22, chicken FKBP65, and chicken CypB

Human and chicken recombinant FKBP22 and CypB were purified from *E. coli* by methods described previously (20, 23). Chicken endogenous FKBP65 was purified from 16-day-old chicken embryos by methods described previously (18).

Purification of collagens

Pepsin-treated native bovine type I and III collagen, hereinafter called full-length, was purified from fetal bovine calf skin by methods described previously (37). Pepsin was inactivated and removed during purification. The carboxyl-terminal quarter fragments of human type III collagen without prolyl 4-hydroxylation was recombinantly expressed using *E. coli* and prepared as described previously (53).

Circular dichroism measurements

Circular dichroism spectra were recorded on an Aviv 202 spectropolarimeter (Aviv, Lakewood, NJ) using a Peltier thermostatted cell holder and a 1-mm path length cell (Starna Cells, Atascadero, CA). Protein concentrations were determined by amino acid analysis. The spectra represent the average of at least 10 scans recorded at a wavelength resolution of 0.1 nm. The proteins were measured in 5 mM Tris/HCl buffer, pH 7.5, containing 0.05 mM $CaCl_2$ at 4 °C. The spectra were analyzed using BestSel (54). The thermal transition curves were measured at 203 nm and 210 nm for FKBP13, the FKBP domain of FKBP19 in PBS, and FKBP22/FKBP23 in 5 mM Tris/HCl buffer, pH 7.2, containing 30 mM $NaCl_2$ and 0.5 mM $CaCl_2$, respectively. Transition curves were monitored as function of temperature with a heating rate of 30 °C/h. Protein concentrations were as follows: 30 μM FKBP13, 45 μM concentrations of FKBP domain of FKBP19, 7 μM FKBP22, and 11 μM FKBP23.

Amino acid sequence comparison between FKBPs

The sequence alignment and similarity were analyzed using the software Vector NTI Advance 11.5.4 (Invitrogen). Protein sequences were obtained from Uniprot, and signal sequence was determined by SignalP 4.1 Server.

Citrate synthase thermal aggregation assay

The aggregation of citrate synthase upon thermal denaturation was measured as reported before (18, 21). Citrate synthase (Sigma) was diluted 200-fold to a final concentration of 0.15 μM into prewarmed 40 mM Hepes buffer, pH 7.4, containing 1 mM $CaCl_2$ at 43 °C. The aggregation of citrate synthase was monitored by absorbance at 500 nm in a Cary Series UV-visible spectrophotometer (Agilent Technologies). All enzyme concentrations were determined by amino acid analysis.

Type I collagen fibril formation assay

Stock solutions of type I collagen in 50 mM acetic acid were diluted to a final concentration of 0.1 μM in 0.1 M sodium bicarbonate buffer, pH 7.8, containing 0.15 M NaCl and 1 mM $CaCl_2$ and 0.15 M sodium phosphate buffer, pH 7.8, containing 0.15 M NaCl for comparisons among FKBPs and for concentration dependence of the FKBP domain of FKBP19, respec-

ASBMB

J. Biol. Chem. (2017) 292(22) 9273–9282 **9279**

tively. Measurements were performed at 34 °C, and the absorbance (light scattering) was monitored at 313 nm as a function of time. All curves are the average of at least three independent measurements.

Refolding of the carboxyl-terminal quarter fragments of type III collagen without prolyl 4-hydroxylation and full-length type III collagen measured by circular dichroism

Refolding of the carboxyl-terminal quarter fragments of type III collagen without prolyl 4-hydroxylation (final concentration, 2.0 μM) and full-length native type III collagen (final concentration, 0.2 μM) were monitored by circular dichroism measurements at 220 nm. Collagens were denatured for 5 min at 45 °C and then added into precooled reaction buffer (50 mM Tris/HCl, pH 7.5, containing 0.2 M NaCl and 1 mM CaCl$_2$) in the presence and absence of PPIases for 4500 s at 25 °C and 5000 s at 10 °C for full-length type III collagen and carboxyl-terminal quarter fragments of type III collagen, respectively. Refolding curves were converted to fraction folded using the amplitude between the native and denatured state of both type III collagen in the absence of PPIases measured by the thermal transition from 5 to 55 °C. All curves are the average of at least three independent measurements.

Preparation of proline-containing substrates

Suc-(A/L)APF-AMC (where Suc and AMC are succinyl and 7-amino-4-methylcoumarin, respectively) were obtained from Peptide Institute, Inc. (Osaka, Japan) and Bachem (Bubendorf, Switzerland), respectively. The Suc-A-(A/L/G)-P-F-pNa peptide and Suc-A-(AO/L-O/G-O/G-Z)-F-pNa peptides (where O is 4-hydroxylproline and Z is 3-hydroxylproline) were purchased from Bachem (Bubendorf, Switzerland) and KareBay Biochem Inc. (Monmouth Junction, NJ), respectively. The stock solutions of substrates were prepared in DMSO, and the final concentrations of AMC, non-hydroxylated pNa, and hydroxylated pNa peptide were 8.8 μM, 75 μM, and 90 μM, respectively. Single capital letters are used as amino acids.

Stopped-flow enzyme assays

Measurements of the catalytic efficiency (k_{cat}/K_m) for the isomerization reaction were performed as described before (25–27). Kinetic measurements were made at 5 °C to minimize the non-enzymatic isomerization reaction in 35 mM HEPES buffer, pH 7.8, containing 1 mM CaCl$_2$. Final substrates of AMC peptide and chymotrypsin concentrations were 8.8 and 12.8 μM, respectively. The final DMSO concentration in the assay was 0.088% and 0.0176% for measurements of A-P and L-P peptides, respectively. For pNa peptides, the final concentrations of chymotrypsin and DMSO were 75 μM and 0.25%, respectively. Fluorescence and absorbance changes were monitored at 380 nm for AMC and at 390 nm for pNa with a HiTech stopped-flow spectrophotometer (TgK Scientific Ltd, Bradford-on-Avon, UK). The assay was started by mixing chymotrypsin and the substrate peptide. Data points were collected using Kinetic Studio version 4.06 software (TgK Scientific), and progression curves were analyzed by fitting to a second-order exponential-decay function with ORIGIN Pro version 9.1 (OriginLab Corp., Northampton, MA). The slower rate of the

decay was used as the *cis*/*trans* isomerization reaction. Values for k_{cat}/K_m were calculated according to $k_{cat}/K_m = (k_{obs} - k_u)/[E]$, where k_u is the rate constant for the uncatalyzed isomerization reaction, and k_{obs} is the rate constant for the catalyzed reaction in the presence of enzymes at a given [E]. k values were calculated using ORIGIN assuming that the reaction consists of two first-order reactions, the fast phase due to the cleavage of the initial *trans* form of X-P/O/Z bond and the slow phase due to the catalyzed or uncatalyzed *cis*-to-*trans* isomerized bond cleavage. The minimum of three independent measurements was preceded for a set of peptide-PPIase. To detect the catalysis, a maximum final concentration of enzyme of 0.5 μM was used in this assay.

Statistical analyses

For comparisons between two groups, we performed one-way analysis of variance to determine whether differences between groups are significant using ORIGIN Pro version. 9.1. The p value <0.05 was considered statistically significant.

References

1. Szabadkai, G., and Rizzuto, R. (2007) Chaperones as parts of organelle networks. *Adv. Exp. Med. Biol.* **594,** 64–77
2. Gidalevitz, T., Stevens, F., and Argon, Y. (2013) Orchestration of secretory protein folding by ER chaperones. *Biochim. Biophys. Acta* **1833,** 2410–2424
3. Hartl, F. U., Bracher, A., and Hayer-Hartl, M. (2011) Molecular chaperones in protein folding and proteostasis. *Nature* **475,** 324–332
4. Braakman, I., and Bulleid, N. J. (2011) Protein folding and modification in the mammalian endoplasmic reticulum. *Annu. Rev. Biochem.* **80,** 71–99
5. Bächinger, H. P., Mizuno, K., Vranka, J. A., and Boudko, S. P. (2010) Collagen formation and structure. In *Comprehensive Natural Products II-Chemistry and Biology* (Mander, L., and Lui, H. W., eds) pp 469–530, Elsevier, Oxford
6. Bateman, J. F., Boot-Handford, R. P., and Lamandé, S. R. (2009) Genetic diseases of connective tissues: cellular and extracellular effects of ECM mutations. *Nat. Rev. Genet.* **10,** 173–183
7. Ishikawa, Y., and Bächinger, H. P. (2013) A molecular ensemble in the rER for procollagen maturation. *Biochim. Biophys. Acta* **1833,** 2479–2491
8. Persikov, A. V., Ramshaw, J. A., Kirkpatrick, A., and Brodsky, B. (2000) Amino acid propensities for the collagen triple-helix. *Biochemistry* **39,** 14960–14967
9. Hudson, D. M., and Eyre, D. R. (2013) Collagen prolyl 3-hydroxylation: a major role for a minor post-translational modification? *Connect Tissue Res.* **54,** 245–251
10. Bächinger, H. P., Bruckner, P., Timpl, R., Prockop, D. J., and Engel, J. (1980) Folding mechanism of the triple helix in type-III collagen and type-III pN-collagen: role of disulfide bridges and peptide bond isomerization. *Eur. J. Biochem.* **106,** 619–632

11. Bella, J. (2016) Collagen structure: new tricks from a very old dog. *Biochem. J.* **473,** 1001–1025

12. Boudko, S. P., Engel, J., and Bächinger, H. P. (2012) The crucial role of trimerization domains in collagen folding. *Int J Biochem. Cell Biol.* **44,** 21–32

13. Bächinger, H. P. (1987) The influence of peptidyl-prolyl cis-trans isomerase on the in vitro folding of type III collagen. *J. Biol. Chem.* **262,** 17144–17148

14. Bächinger, H. P., Bruckner, P., Timpl, R., and Engel, J. (1978) The role of cis-trans isomerization of peptide bonds in the coil leads to and comes from triple helix conversion of collagen. *Eur. J. Biochem.* **90,** 605–613

15. Bruckner, P., and Eikenberry, E. F. (1984) Formation of the triple helix of type I procollagen in cellulo. Temperature-dependent kinetics support a model based on cis in equilibrium trans isomerization of peptide bonds. *Eur. J. Biochem.* **140,** 391–395

16. Bruckner, P., Bächinger, H. P., Timpl, R., and Engel, J. (1978) Three conformationally distinct domains in the amino-terminal segment of type III procollagen and its rapid triple helix leads to and comes from coil transition. *Eur. J. Biochem.* **90,** 595–603

17. Ishikawa, Y., Boudko, S., and Bächinger, H. P. (2015) Ziploc-ing the structure: triple helix formation is coordinated by rough endoplasmic reticulum resident PPIases. *Biochim. Biophys. Acta* **1850,** 1983–1993

18. Ishikawa, Y., Vranka, J., Wirz, J., Nagata, K., and Bächinger, H. P. (2008) The rough endoplasmic reticulum-resident FK506-binding protein FKBP65 is a molecular chaperone that interacts with collagens. *J. Biol. Chem.* **283,** 31584–31590

19. Denessiouk, K., Permyakov, S., Denesyuk, A., Permyakov, E., and Johnson, M. S. (2014) Two structural motifs within canonical EF-hand calcium-binding domains identify five different classes of calcium buffers and sensors. *PLoS ONE* **9,** e109287

20. Ishikawa, Y., and Bächinger, H. P. (2014) A substrate preference for the rough endoplasmic reticulum resident protein FKBP22 during collagen biosynthesis. *J. Biol. Chem.* **289,** 18189–18201

21. Ishikawa, Y., Wirz, J., Vranka, J. A., Nagata, K., and Bächinger, H. P. (2009) Biochemical characterization of the prolyl 3-hydroxylase 1·cartilage-associated protein·cyclophilin B complex. *J. Biol. Chem.* **284,** 17641–17647

22. Islam, M., Gor, J., Perkins, S. J., Ishikawa, Y., Bächinger, H. P., and Hohenester, E. (2013) The concave face of decorin mediates reversible dimerization and collagen binding. *J. Biol. Chem.* **288,** 35526–35533

23. Ishikawa, Y., Vranka, J. A., Boudko, S. P., Pokidysheva, E., Mizuno, K., Zientek, K., Keene, D. R., Rashmir-Raven, A. M., Nagata, K., Winand, N. J., and Bächinger, H. P. (2012) Mutation in cyclophilin B that causes hyperelastosis cutis in American quarter horse does not affect peptidylprolyl cis-trans isomerase activity but shows altered cyclophilin b-protein interactions and affects collagen folding. *J. Biol. Chem.* **287,** 22253–22265

24. Zeng, B., MacDonald, J. R., Bann, J. G., Beck, K., Gambee, J. E., Boswell, B. A., and Bächinger, H. P. (1998) Chicken FK506-binding protein, FKBP65, a member of the FKBP family of peptidylprolyl cis-trans isomerases, is only partially inhibited by FK506. *Biochem. J.* **330,** 109–114

25. Fischer, G., Bang, H., and Mech, C. (1984) Determination of enzymatic catalysis for the cis-trans-isomerization of peptide binding in proline-containing peptides. *Biomed. Biochim. Acta* **43,** 1101–1111

26. Harrison, R. K., and Stein, R. L. (1990) Substrate specificities of the peptidyl prolyl cis-trans isomerase activities of cyclophilin and FK-506 binding protein: evidence for the existence of a family of distinct enzymes. *Biochemistry* **29,** 3813–3816

27. Harrison, R. K., and Stein, R. L. (1990) Mechanistic studies of peptidyl prolyl cis-trans isomerase: evidence for catalysis by distortion. *Biochemistry* **29,** 1684–1689

28. Berg, R. A., and Prockop, D. J. (1973) The thermal transition of a non-hydroxylated form of collagen: evidence for a role for hydroxyproline in stabilizing the triple-helix of collagen. *Biochem. Biophys. Res. Commun.* **52,** 115–120

29. Jimenez, S., Harsch, M., and Rosenbloom, J. (1973) Hydroxyproline stabilizes the triple helix of chick tendon collagen. *Biochem. Biophys. Res. Commun.* **52,** 106–114

30. Rosenbloom, J., Harsch, M., and Jimenez, S. (1973) Hydroxyproline content determines the denaturation temperature of chick tendon collagen. *Arch. Biochem. Biophys.* **158,** 478–484

31. Holster, T., Pakkanen, O., Soininen, R., Sormunen, R., Nokelainen, M., Kivirikko, K. I., and Myllyharju, J. (2007) Loss of assembly of the main basement membrane collagen, type IV, but not fibril-forming collagens and embryonic death in collagen prolyl 4-hydroxylase I null mice. *J. Biol. Chem.* **282,** 2512–2519

32. Pyott, S. M., Schwarze, U., Christiansen, H. E., Pepin, M. G., Leistritz, D. F., Dineen, R., Harris, C., Burton, B. K., Angle, B., Kim, K., Sussman, M. D., Weis, M., Eyre, D. R., Russell, D. W., McCarthy, K. J., Steiner, R. D., and Byers, P. H. (2011) Mutations in PPIB (cyclophilin B) delay type I procollagen chain association and result in perinatal lethal to moderate osteogenesis imperfecta phenotypes. *Hum. Mol. Genet.* **20,** 1595–1609

33. van Dijk, F. S., Nesbitt, I. M., Zwikstra, E. H., Nikkels, P. G., Piersma, S. R., Fratantoni, S. A., Jimenez, C. R., Huizer, M., Morsman, A. C., Cobben, J. M., van Roij, M. H., Elting, M. W., Verbeke, J. I., Wijnaendts, L. C., Shaw, N. J., *et al.* (2009) PPIB mutations cause severe osteogenesis imperfecta. *Am. J. Hum. Genet.* **85,** 521–527

34. Baumann, M., Giunta, C., Krabichler, B., Rüschendorf, F., Zoppi, N., Colombi, M., Bittner, R. E., Quijano-Roy, S., Muntoni, F., Cirak, S., Schreiber, G., Zou, Y., Hu, Y., Romero, N. B., Carlier, R. Y., *et al.* (2012) Mutations in FKBP14 cause a variant of Ehlers-Danlos syndrome with progressive kyphoscoliosis, myopathy, and hearing loss. *Am. J. Hum. Genet.* **90,** 201–216

35. Murray, M. L., Yang, M., Fauth, C., and Byers, P. H. (2014) FKBP14-related Ehlers-Danlos syndrome: expansion of the phenotype to include vascular complications. *Am. J. Med. Genet. A* **164A,** 1750–1755

36. Grafe, I., Yang, T., Alexander, S., Homan, E. P., Lietman, C., Jiang, M. M., Bertin, T., Munivez, E., Chen, Y., Dawson, B., Ishikawa, Y., Weis, M. A., Sampath, T. K., Ambrose, C., Eyre, D., Bächinger, H. P., and Lee, B. (2014) Excessive transforming growth factor-β signaling is a common mechanism in osteogenesis imperfecta. *Nat. Med.* **20,** 670–675

37. Pokidysheva, E., Zientek, K. D., Ishikawa, Y., Mizuno, K., Vranka, J. A., Montgomery, N. T., Keene, D. R., Kawaguchi, T., Okuyama, K., and Bächinger, H. P. (2013) Posttranslational modifications in type I collagen from different tissues extracted from wild type and prolyl 3-hydroxylase 1 null mice. *J. Biol. Chem.* **288,** 24742–24752

38. Yang, C., Park, A. C., Davis, N. A., Russell, J. D., Kim, B., Brand, D. D., Lawrence, M. J., Ge, Y., Westphall, M. S., Coon, J. J., and Greenspan, D. S. (2012) Comprehensive mass spectrometric mapping of the hydroxylated amino acid residues of the alpha1(V) collagen chain. *J. Biol. Chem.* **287,** 40598–40610

39. Gryder, R. M., Lamon, M., and Adams, E. (1975) Sequence position of 3-hydroxyproline in basement membrane collagen. Isolation of glycyl-3-hydroxyprolyl-4-hydroxyproline from swine kidney. *J. Biol. Chem.* **250,** 2470–2474

40. Pokidysheva, E., Boudko, S., Vranka, J., Zientek, K., Maddox, K., Moser, M., Fässler, R., Ware, J., and Bächinger, H. P. (2014) Biological role of prolyl 3-hydroxylation in type IV collagen. *Proc. Natl. Acad. Sci. U.S.A.* **111,** 161–166

41. Basak, T., Vega-Montoto, L., Zimmerman, L. J., Tabb, D. L., Hudson, B. G., and Vanacore, R. M. (2016) Comprehensive characterization of glycosylation and hydroxylation of basement membrane collagen IV by high-resolution mass spectrometry. *J. Proteome Res.* **15,** 245–258

42. Vranka, J. A., Sakai, L. Y., and Bächinger, H. P. (2004) Prolyl 3-hydroxylase 1, enzyme characterization and identification of a novel family of enzymes. *J. Biol. Chem.* **279,** 23615–23621

43. Baldridge, D., Schwarze, U., Morello, R., Lennington, J., Bertin, T. K., Pace, J. M., Pepin, M. G., Weis, M., Eyre, D. R., Walsh, J., Lambert, D., Green, A., Robinson, H., Michelson, M., Houge, G., *et al.* (2008) CRTAP and LEPRE1 mutations in recessive osteogenesis imperfecta. *Hum. Mutat.* **29,** 1435–1442

44. Barnes, A. M., Chang, W., Morello, R., Cabral, W. A., Weis, M., Eyre, D. R., Leikin, S., Makareeva, E., Kuznetsova, N., Uveges, T. E., Ashok, A., Flor, A. W., Mulvihill, J. J., Wilson, P. L., Sundaram, U. T., Lee, B., and Marini, J. C. (2006) Deficiency of cartilage-associated protein in recessive lethal osteogenesis imperfecta. *N. Engl. J. Med.* **355,** 2757–2764

45. Cabral, W. A., Chang, W., Barnes, A. M., Weis, M., Scott, M. A., Leikin, S., Makareeva, E., Kuznetsova, N. V., Rosenbaum, K. N., Tifft, C. J., Bulas, D. I., Kozma, C., Smith, P. A., Eyre, D. R., and Marini, J. C. (2007) Prolyl 3-hydroxylase 1 deficiency causes a recessive metabolic bone disorder resembling lethal/severe osteogenesis imperfecta. *Nat. Genet.* **39,** 359–365

46. Morello, R., Bertin, T. K., Chen, Y., Hicks, J., Tonachini, L., Monticone, M., Castagnola, P., Rauch, F., Glorieux, F. H., Vranka, J., Bächinger, H. P., Pace, J. M., Schwarze, U., Byers, P. H., Weis, M., Fernandes, R. J., *et al.* (2006) CRTAP is required for prolyl 3- hydroxylation and mutations cause recessive osteogenesis imperfecta. *Cell* **127,** 291–304

47. Vranka, J. A., Pokidysheva, E., Hayashi, L., Zientek, K., Mizuno, K., Ishikawa, Y., Maddox, K., Tufa, S., Keene, D. R., Klein, R., and Bächinger, H. P. (2010) Prolyl 3-hydroxylase 1 null mice display abnormalities in fibrillar collagen-rich tissues such as tendons, skin, and bones. *J. Biol. Chem.* **285,** 17253–17262

48. Terajima, M., Taga, Y., Chen, Y., Cabral, W. A., Hou-Fu, G., Srisawasdi, S., Nagasawa, M., Sumida, N., Hattori, S., Kurie, J. M., Marini, J. C., and Yamauchi, M. (2016) Cyclophilin-B modulates collagen cross-linking by differentially affecting lysine hydroxylation in the helical and telopeptidyl domains of tendon type I collagen. *J. Biol. Chem.* **291,** 9501–9512

49. Schmelzer, C. E., Nagel, M. B., Dziomba, S., Merkher, Y., Sivan, S. S., and Heinz, A. (2016) Prolyl hydroxylation in elastin is not random. *Biochim. Biophys. Acta* **1860,** 2169–2177

50. Feige, M. J., Groscurth, S., Marcinowski, M., Shimizu, Y., Kessler, H., Hendershot, L. M., and Buchner, J. (2009) An unfolded CH1 domain controls the assembly and secretion of IgG antibodies. *Mol. Cell* **34,** 569–579

51. Williamson, M. P. (1994) The structure and function of proline-rich regions in proteins. *Biochem. J.* **297,** 249–260

52. Kuo, C. L., Isogai, Z., Keene, D. R., Hazeki, N., Ono, R. N., Sengle, G., Bächinger, H. P., and Sakai, L. Y. (2007) Effects of fibrillin-1 degradation on microfibril ultrastructure. *J. Biol. Chem.* **282,** 4007–4020

53. Mizuno, K., Boudko, S., Engel, J., and Bächinger, H. P. (2013) Vascular Ehlers-Danlos syndrome mutations in type III collagen differently stall the triple helical folding. *J. Biol. Chem.* **288,** 19166–19176

54. Micsonai, A., Wien, F., Kernya, L., Lee, Y. H., Goto, Y., Réfrégiers, M., and Kardos, J. (2015) Accurate secondary structure prediction and fold recognition for circular dichroism spectroscopy. *Proc. Natl. Acad. Sci. U.S.A.* **112,** E3095–E3103

55. Boudko, S. P., Ishikawa, Y., Nix, J., Chapman, M. S., and Bächinger, H. P. (2014) Structure of human peptidyl-prolyl cis-trans isomerase FKBP22 containing two EF-hand motifs. *Protein Sci.* **23,** 67–75